*Published online 7 February 2011* *Nucleic Acids Research, 2011, Vol. 39, No. 7* ***2995–3004***
*doi:10.1093/nar/gkq914*

# Biochemical behavior of *N*-oxidized cytosine and adenine bases in DNA polymerase-mediated primer extension reactions

**Hirosuke Tsunoda, Tomomi Kudo, Yoshiaki Masaki, Akihiro Ohkubo, Kohji Seio and Mitsuo Sekine***

Department of Life Science, Tokyo Institute of Technology and CREST, JST (Japan Science and Technology Agency), 4259 Nagatsuta, Midoriku, Yokohama 226-8501, Japan

Received August 2, 2010; Revised and Accepted September 24, 2010

## ABSTRACT

**To clarify the biochemical behavior of 2′-deoxyribonucleoside 5′-triphosphates and oligodeoxyribonucleotides (ODNs) containing cytosine *N*-oxide ($C^o$) and adenine *N*-oxide ($A^o$), we examined their base recognition ability in DNA duplex formation using melting temperature ($T_m$) experiments and their substrate specificity in DNA polymerase-mediated replication. As the result, it was found that the $T_m$ values of modified DNA–DNA duplexes incorporating 2′-deoxyribonucleoside *N*-oxide derivatives significantly decreased compared with those of the unmodified duplexes. However, single insertion reactions by DNA polymerases of Klenow fragment (KF) ($exo^-$) and Vent ($exo^-$) suggested that $C^o$ and $A^o$ selectively recognized G and T, respectively. Meanwhile, the kinetic study showed that the incorporation efficiencies of the modified bases were lower than those of natural bases. *Ab initio* calculations suggest that these modified bases can form the stable base pairs with the original complementary bases. These results indicate that the modified bases usually recognize the original bases as partners for base pairing, except for misrecognition of dATP by the action of KF ($exo^-$) toward $A^o$ on the template, and the primers could be extended on the template DNA. When they misrecognized wrong bases, the chain could not be elongated so that the modified base served as the chain terminator.**

## INTRODUCTION

DNA bases are oxidized by reactive oxygen species (ROS) in the living body. Reactions of ROS with pyrimidine and purine bases result in the formation of several types of oxidation products in genomic DNA (1–7). For example, 5,6-dihydroxy-5,6-dihydrothymine (thymine glycol) and 5,6-dihydroxy-5,6-dihydrouracil (uracil glycol) are generated by the reactions of the hydroxyl radical, which is most mediated in the oxidation reactions, with pyrimidine bases. Additionally, the oxidation of guanine by singlet oxygen produces 8-oxo-7,8-dihydroguanine as a major oxidation product of guanine. These modifications have been found to block the chain elongation by DNA polymerases or to lead mutations (8–10). Oxidation by ROS occurs not only in genomic DNA, but also in the nucleotide pool. In fact, the reactions of dNTPs with ROS in the nucleotide pool were reported to produce oxidized dNTP derivatives, such as 8-oxo-7,8-dihydroguanosine 5′-triphosphate (11,12). The oxidized dNTP derivatives were incorporated into the growing chains on DNA templates using DNA polymerases in DNA replication and cause mutation or inhibition of chain elongation (13–15). Consequently, DNA base oxidation has been recognized as a major cause of genetic mutations that play an important role in many biological processes, such as cancers, aging, and genetic diseases (16–18).

Hydrogen peroxide, which is a more unreactive ROS than hydroxyl radical, is important in understanding the mechanism of oxidatively DNA damage. It is a major non-radical species produced by a series of metabolic processes of non-reactive superoxide anions, and is widely present in living cells (19–21). The main products obtained by the oxidation of cytosine and adenine bases with hydrogen peroxide are cytosine *N*-oxide ($C^o$) and adenine *N*-oxide ($A^o$) derivatives, respectively (Figure 1) (22–32).

Cadet reported that adenine $N^1$-oxide is formed using hydrogen peroxide as a predominant ionic DNA base damage under non-radical conditions (29). 2′-Deoxyadenosine $N^1$-oxide ($3.2/10^6$ bases) was detected to be present in the DNA of the untreated wild-type *Proteus mirabilis* cells (28). When they were exposed to

*To whom correspondence should be addressed. Tel: +81 45 924 5706; Fax: +81 45 924 5772; Email: msekine@bio.titech.ac.jp


**Figure 1.** Structures of A° and C° derivatives.

nonlethal level of 10 mM hydrogen peroxide, the amount of this modified nucleoside was found to be 8.3 times higher than in the untreated cells (28). Upon exposure of calf thymus DNA to 10 mM hydrogen peroxide for 30 min, the number of the oxidized adenine residues was reported to be $0.7/10^4$ bases. If this oxidative reaction of dCTP and dATP with hydrogen peroxide occurs in the nucleotide pool, the corresponding 2′-deoxyribonucleoside *N*-oxide 5′-triphosphates would be incorporated into DNA duplexes using DNA polymerases in DNA replication. Because these *N*-oxide derivatives have an additional oxygen atom at the Watson–Crick base pairing site, their hydrogen bond formation could be different from the normal ones. Therefore, there is a possibility that these 2′-deoxyribonucleoside *N*-oxides are mutagenic in DNA replication, such as the well-known 8-oxo-7,8-dihydroguanine (33). In addition, 2′-deoxyribonucleoside *N*-oxides might have a harmful effect on DNA transcription and replication.

It is known that 2′-deoxyribonucleoside *N*-oxide derivatives have some biological activities. Brown *et al*. (34) previously reported strong growth-inhibitory activity of adenosine $N^1$-oxide and AMP $N^1$-oxide in mouse sarcoma 180 cells. Adenine $N^1$-oxide was converted into 2-hydroxyadenine by ultraviolet radiation (35). Its photochemical conversion might occur in skin as a rather minor process. In addition, it has been reported that adenosine $N^1$-oxide was a highly selective inhibitor of vaccinia virus replication and viral late protein synthesis (36,37). Because 2′-deoxycytidine is readily oxidized to the $N^3$-oxide derivative by treatment with hydrogen peroxide, it seems possible that the cytosine $N^3$-oxide base forms in DNA upon treatment with hydrogen peroxide; however, this modified species has not been isolated from the oxidatively damaged DNA. The objective of this study is to examine the base recognition abilities of 2′-deoxyribonucleoside *N*-oxide moieties in DNA polymerase reactions to clarify their longstanding unknown biological properties.

In our previous study, we reported the synthesis of oligodeoxyribonucleotides (ODNs) containing 2′-deoxyribonucleoside *N*-oxide derivatives using a post-synthetic modification method (38). In this article, we report the base recognition abilities of C° and A° bases by $T_m$ experiments using synthetic ODNs incorporating them. We also report the substrate specificity of 2′-deoxyribonucleoside *N*-oxide derivatives in primer extension reactions using various DNA polymerases, i.e. not only in incorporation of dC°TP or dA°TP into DNA primers on DNA templates but also in incorporation of dNTP into DNA primers in DNA templates containing C° or A°. In addition, the base recognition abilities of C° and A° are also discussed on the basis of the hydrogen bond energies resulting from their *ab initio* calculations and MD simulations.

## MATERIALS AND METHODS

### General remarks

$^1$H and $^{31}$P NMR spectra were recorded at 270 and 109 MHz, respectively. The chemical shifts were measured from tetramethylsilane for $^1$H NMR spectra and 85% phosphoric acid (0 ppm) for $^{31}$P NMR spectra. UV spectra were recorded on a U-2000 spectrometer. High-performance liquid chromatography (HPLC) was performed using the following systems. Reversed-phase HPLC was done on a system with a 3D UV detector and a C18 column ($4.6 \times 150$ mm). A linear gradient (0–30%) of solvent I [0.03 M ammonium acetate buffer (pH 7.0)] in solvent II ($CH_3CN$) was used at 30°C at a rate of 1.0 ml/min for 30 min. DEAE–HPLC was performed on a Waters Alliance system with a Waters 3D UV detector and a Shodex DEAE column ($8 \times 75$ mm). A linear gradient (0–45%) of solvent III [50 mM triethylammonium bicarbonate buffer (pH 7.2)] in solvent IV [500 mM triethylammonium bicarbonate buffer (pH 7.2)] was used at 25°C at a rate of 1.0 ml/min for 35 min. ESI mass was performed using Mariner™ (PerSeptive Biosystems Inc.). MALDI-TOF mass spectroscopy was performed using Bruker Daltonics [Matrix: 3-hydroxypicolinic acid (100 mg/ml) in $H_2O$-diammoniumhydrogen citrate (100 mg/ml) in $H_2O$ (10:1, v/v)]. Highly cross-linked polystyrene (HCP) was purchased from ABI. DNA polymerase I Klenow fragment ($exo^-$) was purchased from Promega. DNA polymerase I Klenow fragment ($exo^+$), Pyrobest polymerase, and dNTPs were purchased from Takara Bio, Inc. Vent ($exo^-$) DNA polymerase was purchased from New England Biolabs, Inc. ODNs used in the enzyme reactions and $T_m$ experiments were purchased from Sigma-Aldrich Japan. 2′-Deoxyribonucleoside *N*-oxide 5′-triphosphates and ODNs containing the *N*-oxidized derivatives were synthesized, as described in Supplementary Data.

### $T_m$ experiments

ODNs containing 2′-deoxyribonucleoside *N*-oxides were synthesized by the post-synthetic oxidation method (38). An appropriate ODN (2 μM) and its complementary 2 μM ssDNA 14-mer or ssRNA 14-mer were dissolved in a buffer consisting of 1 M NaCl, 10 mM sodium phosphate and 0.1 mM EDTA adjusted to pH 7.0. The solution was maintained at 80°C for 10 min for complete dissociation of the duplex to single strands, cooled to 5°C at the rate of 0.5°C/min and heated to 80°C at the same rate using UV-1700™ (Shimadzu). During this annealing and melting, the absorption at 260 nm was recorded and used to draw UV melting curves. The $T_m$ value was calculated as the temperature at which the first derivative of the UV melting curve had a maximum.

### Single dNTP insertion reaction using Klenow fragment (exo$^-$) DNA polymerase

The reaction mixture (10 μl) contained 50 mM Tris–HCl (pH 7.2), 10 mM $MgSO_4$, 0.1 mM DTT, 100 nM 5′-FAM-labeled primer/template, 0.1 U enzyme and 10 μM dNTP ($N$ = A$^o$, C$^o$, A, G, C or T). The mixture was incubated at 37°C for 10 min, and the reactions were terminated by adding 30 μl of stop solution (98% formamide, 20 mM EDTA). After being vortexed gently, the samples were separated by electrophoresis using 20% denaturing polyacrylamide gel containing 7 M urea and were fluorescently visualized by Fujifilm FLA-2000G or FLA-7000. These results are shown in Supplementary Figures S1 and S3. The reactions using other enzymes were described in Supplementary Data.

### Extension reactions of the primer with dNTPs in the presence or absence of dA$^o$TP or dC$^o$TP on templates composed of only natural bases or involving A$^o$ or C$^o$

Extension reactions were performed under the same conditions as described above for Klenow fragment (exo$^-$) DNA polymerase or Vent (exo$^-$) DNA polymerase, except that the reactions were performed in the presence of three or four of dGTP, dTTP, dATP and dCTP (if necessary dA$^o$TP, or dC$^o$TP) (each dNTP at 10 μM). These results are shown in Figures 2 and 3 in the text.

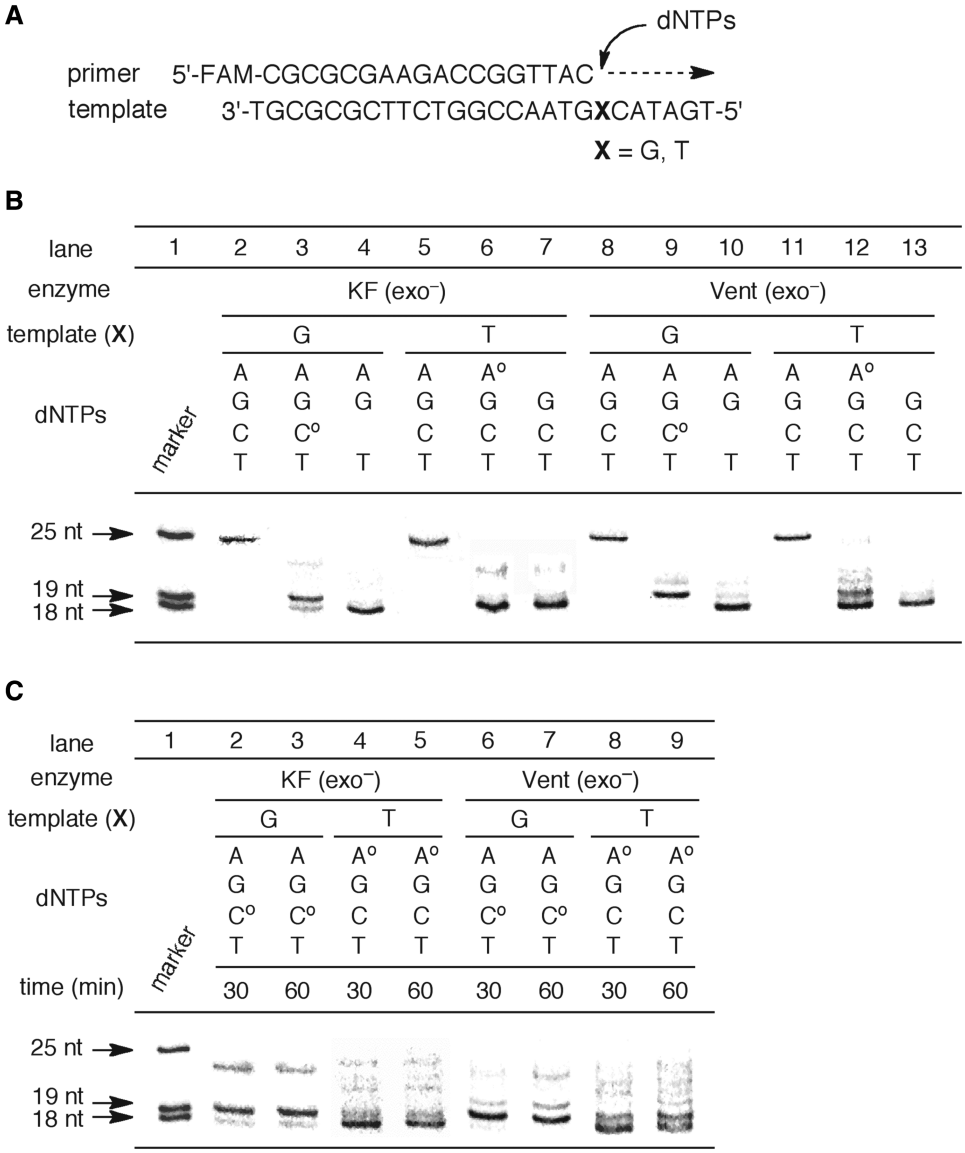


**Figure 2.** Extension reactions with mixed dNTPs. (**A**) Sequences of 5′-FAM labeled 18-nt primer and 26-nt templates. (**B**) PAGE analysis of extension reactions using the natural and oxidized dNTPs (each dNTP at 10 μM) in the natural template. Lane 1 refers to the appropriate size markers. (**C**) Extension reactions in the presence of dGTP, dTTP, dATP and dC$^o$TP (each dNTP at 10 μM) were shown in lanes 2 and 3 by KF (exo$^-$) and lanes 6 and 7 by Vent (exo$^-$). Extension reactions in the presence of dGTP, dTTP, dCTP and dA$^o$TP (each dNTP at 10 μM) were shown in lanes 4 and 5 by KF (exo$^-$) and lanes 8 anmd 9 by Vent (exo$^-$). Lane 1 refer to the appropriate marker.

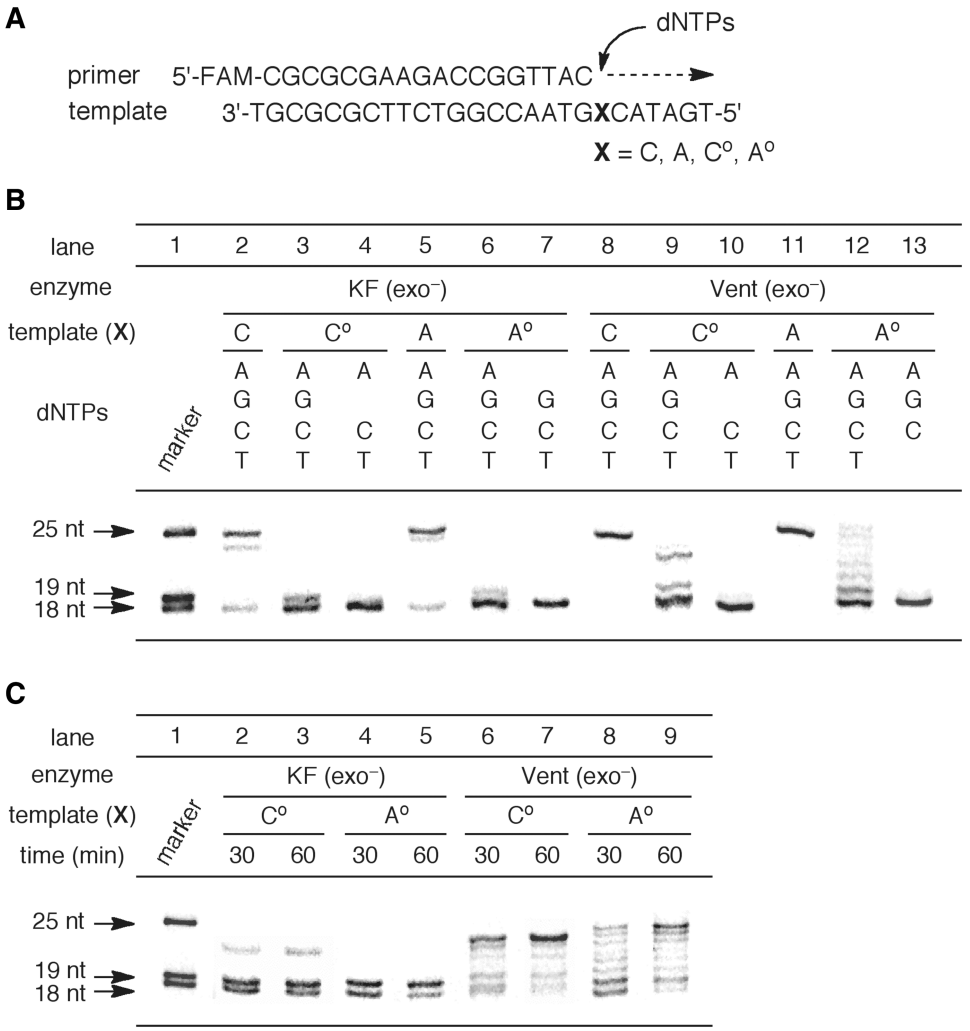


**Figure 3.** Extension reactions with mixed dNTPs. (**A**) Sequences of 5′-FAM labeled 18-nt primer and 26-nt templates. (**B**) PAGE analysis of extension reactions using mixed dNTPs (each dNTP at 10 μM) in the oxidized templates. Lanes 1 refers to the appropriate marker. (**C**) PAGE analysis of extension reactions in the presence of dGTP, dTTP, dATP and dCTP (each dNTP at 10 μM). Lane 1 refer to the appropriate marker. Extension reactions by KF (exo$^-$) are shown in lanes 2–5, and its reactions by Vent (exo$^-$) are shown in lanes 6–9.

The results obtained when the reaction time was elongated to 30 or 60 min are also shown in Figures 2 and 3.

### Steady-state kinetics methods in reactions using oxidized dNTPs and natural templates

A reaction mixture (10 μl) of 10 mM $MgSO_4$, 0.1 mM DTT, 100 nM 5′-FAM-labeled primer/template duplex having the sequence [5′-FAM-(CGCGCGAAGACCG GTTAC)-3′/5′-(TAAGACXGTAACCGGTCTTCGCGC G)-3′, X = A, G, C and T], DNA polymerase Klenow fragment (exo$^-$), dNTP (N = A°, C°, A or C) in 50 mM Tris–HCl (pH 7.2) was incubated at 37°C for the appropriate times. The concentration of dNTP (0.2–50 μM) and the reaction time were adjusted for each reaction so as to give the product yield of ≤25%. The reactions were terminated by adding 30 μl of a stop solution (98% formamide, 20 mM EDTA). After being vortexed gently, the reactions were analyzed by electrophoresis with 20% denaturing polyacrylamide gel containing 7 M urea. The reactions were monitored with Fujifilm FLA-2000G. Relative velocity $v$ was measured as the ratio of the extended product ($I_{ext}$) to the remaining primer ($I_{prim}$) using $v = I_{ext}/I_{prim}\ t$, where $t$ represents the reaction time, and normalized for the lowest enzyme concentration used. The kinetic parameters ($K_m$ and $V_{max}$) were obtained from Hanes–Woolf plots. Each parameter was averaged from three data sets. These results are shown in Table 1. Steady-state kinetics methods in reactions using natural dNTPs and oxidized templates were described in Supplementary Data.

## RESULTS AND DISCUSSION

### $T_m$ experiment

To clarify the base pairing properties of the C° and A° bases in DNA duplexes, $T_m$ experiments were performed using duplexes formed between modified ODNs and their complementary ODNs with matched or single-mismatched sequences at the central position (Supplementary Table S1). An unmodified duplex of

**Table 1.** Steady-state kinetic parameters for the insertion of single nucleotides into a template–primer duplex by Klenow fragment (exo$^-$)[a]

| dNTP | Template (X) | $K_m$ (μM) | $V_{max}$[b] (percentage per minute) | Efficiency ($V_{max}/K_m$) |
|---|---|---|---|---|
| $C^o$ | G | 1.2 (0.30) | 0.083 (0.016) | $6.9 \times 10^4$ |
| $C^o$ | A | 53 (14) | 0.006 (0.001) | $1.0 \times 10^2$ |
| $C^o$ | C | ND[c] | ND[c] | $<1.0 \times 10^2$ |
| $C^o$ | T | ND[c] | ND[c] | $<1.0 \times 10^2$ |
| C | G | 0.25 (0.16) | 0.51 (0.11) | $2.0 \times 10^6$ |
| $A^o$ | T | 1.2 (0.41) | 0.060 (0.001) | $4.9 \times 10^4$ |
| $A^o$ | G | 15 (3.2) | 0.059 (0.015) | $3.8 \times 10^3$ |
| $A^o$ | C | 14 (2.9) | 0.008 (0.001) | $5.3 \times 10^2$ |
| $A^o$ | A | ND[c] | ND[c] | $<1.0 \times 10^2$ |
| A | T | 0.11 (0.020) | 0.36 (0.027) | $3.2 \times 10^6$ |

[a]Assay was carried out at 37°C for 0.5–5 min using 100 nM template–primer duplex, 0.05–1 U enzyme and 0.2–50 μM dNTP in a solution (10 μl) containing 50 mM Tris–HCl (pH 7.2), 10 mM $MgSO_4$ and 0.1 mM DTT. The values in parenthesis are standard deviations.
[b]Normalized for the lowest enzyme concentration used.
[c]Not determined. No inserted products were detected after incubation for 10 min with 50 μM dNTP.

$dA_7GA_6/dT_6CT_7$ with a matched natural C–G base pair showed a $T_m$ value of 47.1°C. In contrast, the $T_m$ value of a duplex with an oxidized $C^o$–G base pair decreased to 30.5°C with a significant drop of 16.6°C compared with the natural C–G matched base pair. In addition, the $T_m$ values of DNA duplexes containing the mismatched pairs such as $C^o$–T and $C^o$–C also decreased. This result indicated that the base pairs of $C^o$–T and $C^o$–C were less stable by ($\Delta T_m$ =) −3.3°C and −3.1°C than the canonical C–T and C–C mismatched base pairs, respectively. However, the DNA duplex containing a $C^o$–A mismatched base pair showed a slightly decreased $T_m$ value ($\Delta T_m$ = −0.6°C) compared with that containing a C–A mismatch, which to our surprise, had the highest $T_m$ value among the four base pairs. The DNA duplexes containing $A^o$ exhibited a tendency similar to those having $C^o$, as shown in Supplementary Table S1. The $T_m$ value of a DNA duplex with an oxidized $A^o$–T base pair decreased by 11.5°C compared to that containing the natural A–T base pair, whereas the base pairs of $A^o$ with G and C resulted in a decrease of 4.0–5.3°C in the $T_m$ values of their duplexes. In the case of $A^o$, the combination of $A^o$ with A gave in the highest $T_m$, similar to the $C^o$–A base pair.

Next, similar $T_m$ experiments were performed using duplexes formed between the modified ODNs and the complementary RNAs with a matched or single-mismatched sequence (Supplementary Table S2). The DNA–RNA duplexes having a $C^o$–G or $A^o$–U base pair proved to be significantly destabilized, as described in the case of the modified DNA–DNA duplexes.

### Synthesis of *N*-oxidized oligodeoxyribonucleotides and 2′-deoxyribonucleoside 5′-triphosphates

To examine the properties of 2′-deoxyribonucleoside *N*-oxide derivatives as substrates in the enzyme reactions, we synthesized $dC^oTP$ and $dA^oTP$ from dCTP and dATP, respectively. These modified 2′-deoxyribonucleoside 5′-triphosphates were easily obtained by treatment of dCTP or dATP with mCPBA in a mixed solvent of MeOH and $NaHCO_3$ aqueous solution (Scheme 1). Consequently, these *N*-oxidation reactions proceeded very efficiently to yield the *N*-oxide derivatives as single products.

We also synthesized ODNs containing $C^o$ and $A^o$ as templates in the enzyme reaction to clarify the base recognition abilities of the *N*-oxidized bases. These template ODNs containing $C^o$ and $A^o$ were obtained by post-synthetic modification in 43% and 43% yields, respectively (Scheme 2) (38).

### Single dNTP insertion by Klenow fragment (exo$^-$)

To study the template-specific incorporation of these 2′-deoxyribonucleoside *N*-oxide 5′-triphosphates using DNA polymerase, we examined single nucleoside insertion reaction using the Klenow fragment (exo$^-$) [KF (exo$^-$)], which lacks the 3′- to 5′-exonuclease activity. The template incorporating one of the four natural bases (A, G, C and T) at position X was annealed with a 5′-FAM-labeled 18-nt primer in the presence of KF (exo$^-$) and $dC^oTP$ or dCTP (Supplementary Figure S1A). After the enzymatic reaction, the products were analyzed by PAGE, as shown in Supplementary Figure S1B. Consequently, $dC^oTP$ was incorporated when X was G, as in the case of dCTP. Moreover, it was revealed that $dC^oTP$ was not incorporated at all when X was A, C or T. Similarly, the incorporation of $dA^oTP$ occurred at the opposite site of the parent T base in the template more precisely than that of dATP (lanes 6 and 8 versus 14 and 16). In the latter, wrong incorporation was observed when X was A or C. These results clearly suggested that 'the $C^o$ and $A^o$ bases could be incorporated accurately into the 3′-terminus of the primers according to the Watson–Crick base pairing rule even after *N*-oxidation', although the above mentioned $T_m$ experiments showed that these $C^o$ and $A^o$ bases exhibited low base pairing abilities toward the original complementary G and T bases, respectively.

To investigate the incorporation efficiencies of the 2′-deoxyribonucleoside *N*-oxide 5′-triphosphates in more detail, we calculated steady-state kinetic parameters for the single insertion reaction using KF (exo$^-$). The results are shown in Table 1. The $V_{max}/K_m$ values in the primer-mediated incorporation of $dC^oTP$ at four opposite natural bases (A, G, C and T) in the templates were determined. As a result, the incorporation efficiency of $dC^oTP$ toward the opposite G in the template was found to be 690-fold higher than that of $dC^oTP$ toward the opposite A. This result shows that $dC^oTP$ is exclusively incorporated into the opposite site of G in the template. It was also suggested that if $dC^oTP$ was produced by the *N*-oxidation of dCTP in nucleotide pool, $dC^oTP$ having high fidelity would be rather selectively incorporated into elongating primers in a manner similar to that of dCTP in the replication. $dA^oTP$ also showed ~13-fold higher selectivity for T than the other bases. The incorporation efficiencies of $dC^oTP$ or dCTP at the opposite site of G as well as $dA^oTP$ or dATP at the opposite site of T were

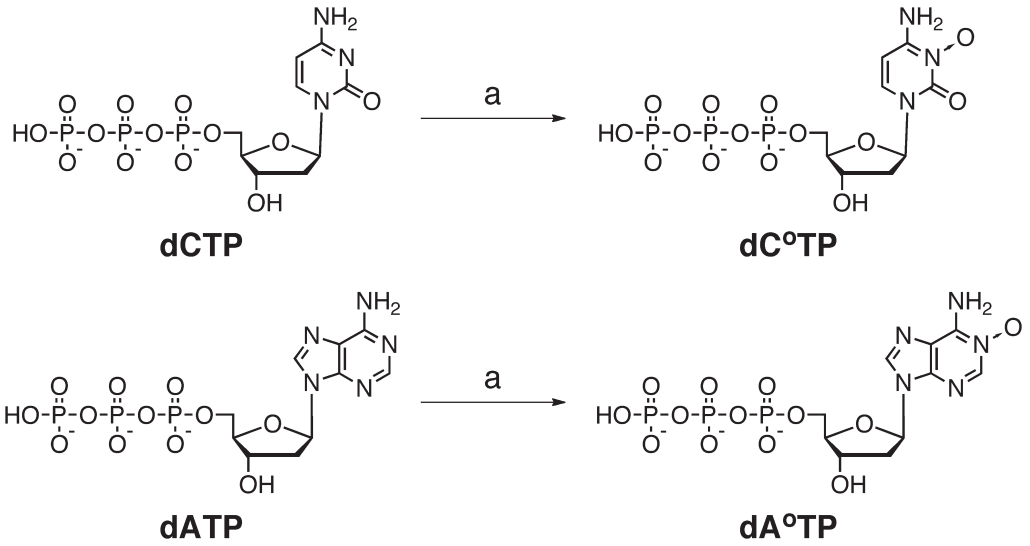


**Scheme 1.** Synthesis of 2′-deoxycytidine and 2′-deoxyadenosine *N*-oxide 5′-triphosphates. Reagents and conditions: (a) mCPBA, aqueous $NaHCO_3$-MeOH (1:1, v/v), rt, 6 h, 42% (for dC°TP), 48% (for dA°TP).

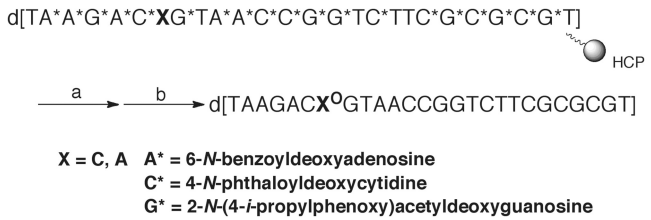


**Scheme 2.** Synthesis of ODNs containing C° and A°. Reagents and conditions: (a) mCPBA, MeOH, rt, 1 h, (b) concentrated $NH_3$ aq, rt, 18 h, 43% (for ODN containing C°), 43% (for ODN containing A°).

extensively studied. Consequently, the $V_{max}/K_m$ values of dC°TP, dCTP, dA°TP and dATP were calculated to be $6.9 \times 10^4$, $2.0 \times 10^6$, $4.9 \times 10^4$ and $3.2 \times 10^6$, respectively. Thus, the incorporation efficiency of oxidized dC°TP in the growing chain was ~29-fold lower than that of dCTP. In addition, dA°TP was incorporated ~65-fold less efficiently than dATP.

### Single dNTP insertion reaction using other polymerases

To clarify the incorporation using other polymerases and the effect of their 3′- to 5′-exonuclease activity, we examined single insertion reactions using Klenow fragment (exo$^+$) [KF (exo$^+$)], Vent (exo$^-$) polymerase and Pyrobest polymerase. Vent (exo$^-$) polymerase and Pyrobest polymerase have been used as well known thermostable enzymes in PCR reactions (39). The former has no proofreading activity like KF (exo$^-$), while the latter has a proofreading activity. The templates and primer used in this study and the results are shown in Supplementary Figure S2.

Supplementary Figure S2B shows the single dNTP-insertion reactions using Vent (exo$^-$) polymerase. dC°TP and dA°TP were preferentially incorporated in a manner similar to that described in the reaction using KF (exo$^-$). The PAGE image of the enzymatic reactions using KF (exo$^+$) is shown in Supplementary Figure S2C. Although KF (exo$^+$) has a 3′- to 5′-exonuclease activity, the 19-nt product containing dC° was explicitly observed when dC°TP was employed (lane 3). The control experiment of dCTP also showed a similar result. When dA°TP was used, it was incorporated at the opposite site of the T residue in the template to give the 19-nt product containing dA° (lane 13). As far as the substrate fidelity was concerned, we observed that dA°TP gave better results than dATP (lanes 10–12 versus 14–16). Regardless of the presence or absence of the exonuclease activity, this tendency was commonly observed in the case of KF (exo$^+$) and KF (exo$^-$), as mentioned above.

In sharp contrast to these results, the 19-nt products containing the *N*-oxide bases were not observed in the single-insertion reactions using Pyrobest polymerase, as shown in Supplementary Figure S2D. In this case, it is likely that even when the *N*-oxide bases were incorporated into the 3′-terminus of the primer, they were removed by the excellent 3′- to 5′-exonuclease activity of Pyrobest polymerase (39). Otherwise, there is a possibility that this enzyme did not recognize the modified bases at all.

### Primer extension reactions using mixed dNTPs involving dC°TP or dA°TP

We performed the full-length extension reactions using KF (exo$^-$) and Vent (exo$^-$) in the presence of a mixture of dNTPs involving dC°TP or dA°TP. The results are

**Table 2.** Steady-state kinetic parameters for the insertion of single nucleotide into a template–primer duplex by KF (exo$^-$), and Vent (exo$^-$)

| Template base (X) | dNTP (N) | KF (exo$^-$)[a] | | | Vent (exo$^-$)[b] | | |
|---|---|---|---|---|---|---|---|
| | | $K_m$ (μM) | $V_{max}$ (percentage per minute) | Efficiency ($V_{max}/K_m$) | $K_m$ (μM) | $V_{max}$ (percentage per minute) | Efficiency ($V_{max}/K_m$) |
| $C^o$ | G | 0.68 (0.20) | 0.18 (0.020) | $2.7 \times 10^5$ | 2.0 (0.19) | 0.81 (0.043) | $4.1 \times 10^5$ |
| $C^o$ | A | 30 (2.5) | 0.024 (0.002) | $8.2 \times 10^2$ | 8.3 (1.1) | 0.017 (0.001) | $2.0 \times 10^3$ |
| $C^o$ | C | ND[c] | ND[c] | $<1.8 \times 10^2$ | ND[c] | ND[c] | $<1.5 \times 10^3$ |
| $C^o$ | T | ND[c] | ND[c] | $<1.8 \times 10^2$ | ND[c] | ND[c] | $<1.5 \times 10^3$ |
| C | G | 0.031 (0.012) | 0.92 (0.056) | $3.0 \times 10^7$ | 0.084 (0.018) | 0.55 (0.029) | $6.6 \times 10^6$ |
| $A^o$ | A | 6.6 (0.94) | 0.061 (0.002) | $9.2 \times 10^3$ | 12 (2.9) | 0.019 (0.001) | $1.5 \times 10^3$ |
| $A^o$ | T | 61 (13) | 0.019 (0.001) | $3.2 \times 10^2$ | 2.0 (1.4) | 0.059 (0.007) | $2.9 \times 10^4$ |
| $A^o$ | C | 130 (28) | 0.024 (0.001) | $1.8 \times 10^2$ | ND[c] | ND[c] | $<1.5 \times 10^3$ |
| $A^o$ | G | ND[c] | ND[c] | $<1.8 \times 10^2$ | ND[c] | ND[c] | $<1.5 \times 10^3$ |
| A | T | – | – | – | 0.45 (0.17) | 2.05 (0.49) | $4.6 \times 10^6$ |

[a]Assay was carried out at 37°C for 0.25–10 min using 100 nM template–primer duplex, 0.05 U enzyme and 0.1–500 μM dNTP in a solution (10 μl) containing 50 mM Tris–HCl (pH 7.2), 10 mM $MgSO_4$ and 0.1 mM DTT.
[b]Assay was carried out at 74°C for 0.25–10 min using 100 nM template–primer duplex, 0.1 U enzyme and 0.05–50 μM dNTP in a solution (10 μl) 20 mM Tris–HCl (pH 8.8), 10 mM $(NH_4)_2SO_4$, 10 mM KCl, 2 mM $MgSO_4$ and 0.1% Triton X-100. The values in parenthesis are standard deviations.
[c]Not determined. No inserted products were detected after incubation for 10 min with 1000 μM dNTP.

summarized in Figure 2B. The KF (exo$^-$)-catalyzed primer extension using a mixture of dNTPs containing $dC^oTP$ on the template, where X was G, yielded mainly the one-base elongated 19-nt product that has $dC^o$, but no full-length 25-nt product was observed. However, we observed an elongation product as a faint band at the position corresponding to 23-mer (lane 3). The formation of this product was explained in terms of consecutive addition of a $C^oGTAT$ sequence after the 3′-terminal site of the primer followed by termination at the second position (G) from the 5′-terminus of the template due to less effective incorporation of $C^o$. Compared with these results, when X was T, the incorporation experiment with $dA^oTP$ gave a somewhat complicated PAGE pattern that was similar to the control without $A^oTP$ (lanes 6 and 7). This is because the part of the single strand on the template involves three T bases so that chain termination occurred at these positions (18, 21 and 24 nt) because of the poor incorporation efficiency of $dA^oTP$ (lane 6) and the absence of $dA^oTP$ (lane 7) after incorporation of the first $A^o$ or misincorporation of the other bases. The elongated products in these primer extensions were more clearly observed when the reaction time was elongated from 10 to 60 min, as shown in Figure 2C. These results reflected that the incorporation efficiency of $dA^oTP$ was very poor.

In the case of Vent (exo$^-$), the use of a mixture of dNTPs containing $dC^oTP$ (X = G) resulted in the formation of the one-nucleotide extended product as the minor band in PAGE (lane 9), while the use of a mixture of dNTPs containing $dA^oTP$ gave a result similar to that obtained by KF (exo$^-$) (lanes 6 versus 12).

Therefore, it was concluded that both enzymes of KF (exo$^-$) and Vent (exo$^-$) allowed incorporation of $dC^oTP$ and $dA^oTP$ at the 3′-terminus of the primer. However, the presence of the once incorporated $dC^o$ or $dA^o$ residue, particularly the former, at the 3′-terminal site of the primer retarded significantly the incorporation of the next dNTP by the DNA polymerase. These properties could have a significant influence on the DNA replication process in living cells when $dC^oTP$ and $dA^oTP$ are produced by the oxidation of dCTP and dATP with $H_2O_2$ in the nucleotide pool.

### Single-nucleotide-insertion reactions of dNTPs toward the opposite $C^o$ or $A^o$ incorporated into DNA templates

Next, we performed the single-insertion reaction of dNTP toward the opposite $C^o$ or $A^o$ in templates using DNA polymerases (Supplementary Figure S3). When X was $C^o$, dGTP was selectively incorporated into the opposite position of $C^o$ in the template by use of KF (exo$^-$) and Vent (exo$^-$). Similar results were obtained when C was used as X. In addition, in order to examine the incorporation efficiencies of the natural dNTPs at the opposite *N*-oxidized base in the templates, we calculated the steady-state kinetic parameters of these reactions. The results are summarized in Table 2.

The incorporation efficiency of dGTP at the opposite $C^o$ in the reaction using KF (exo$^-$) indicated at least ~330-fold higher value than those of the other dNTPs. Moreover, in the reaction using Vent (exo$^-$), its incorporation efficiency was at least ~205-fold higher than those of the other dNTPs at the opposite $C^o$. Therefore, it was found that dGTP was rather selectively chosen from the four natural dNTPs as the complementary base for $C^o$. The $V_{max}/K_m$ values of dGTP at the opposite C and $C^o$ were $3.0 \times 10^7$ and $2.7 \times 10^5$, respectively, in the case of KF (exo$^-$). The incorporation efficiency of dGTP at the oxidized $C^o$ was significantly lower by two orders than that of dGTP at the natural C.

On the other hand, we obtained interesting results in the insertion reaction using the template having $A^o$. When Vent (exo$^-$) was employed, dTTP was predominantly incorporated into the site opposite $A^o$ over dTTP in a manner similar to that of the natural A. To our surprise, when KF (exo$^-$) was used, dATP was more preferentially incorporated into the opposite position of $A^o$ in the

template than dTTP. The $V_{max}/K_m$ value of dATP ($9.2 \times 10^3$) was ~30-fold higher than that of dTTP ($3.2 \times 10^2$), as shown in Table 2. Therefore, if $A^o$ is produced by the *N*-oxidation of the adenine base in DNA genome or $A^o$ is incorporated into DNA genome by $A^o$TP-mediated replications, an $A^o$–A mismatch base pair might be formed in the DNA replication process. Its mismatch base pair would cause a significant transversion mutation to induce genetic diseases.

In addition, we carried out the insertion reactions using KF (exo$^+$) and Pyrobest (Supplementary Figure S3). KF (exo$^+$) incorporated not only dGTP as a match substrate, but also dATP as a mismatch substrate into the site opposite $C^o$. In the template containing $A^o$, similar mis-incorporation of dATP was observed. Considering the results using KF (exo$^-$), Klenow fragment tends to have an ability of incorporation of dATP into the opposite site of *N*-oxide bases in the template. In the reactions using Pyrobest, dGTP and dTTP were slightly incorporated into the opposite $C^o$ and $A^o$, respectively.

### Primer extension reactions with mixed dNTPs

Next, we performed the full-length extension reactions using KF (exo$^-$) or Vent (exo$^-$) in the presence of various mixtures of dNTPs and the templates containing $C^o$ or $A^o$, as shown in Figure 3B. In the case of KF (exo$^-$), the extension of the primer was stopped after the incorporation of dGTP and dATP at the opposite $C^o$ and $A^o$, respectively, in the template (lanes 3 and 6). Thus, the 2′-deoxyribonucleoside *N*-oxide residues in the templates showed very strong inhibition in the elongation of the primer by KF (exo$^-$). This inherent property would interrupt the DNA-replication process, and thus prevent precise genetic information from transferring to new genomic DNA.

In contrast, the enymatic reactions using Vent (exo$^-$) showed interesting results different from those derived from KF (exo$^-$). It turned out that Vent (exo$^-$) could extend the primer over $C^o$ or $A^o$ in the template to give elongated primers, although these reactions generated shorter extension products than the full-length products (lanes 9 and 12).

We also examined in more detail the extension reactions under the conditions of prolonged reaction time to clarify whether longer products were generated (Figure 3C). As the result, the prolonged reaction using the template containing $A^o$ gave the 25-nt full length DNA oligomer as the major product. Using the template containing $C^o$, we observed a 24-nt main product probably lacking the A residue at the 3′-terminal position of the primer. It is unclear why such a truncated oligomer was formed.

Therefore, we found that the enzymatic behavior of 2′-deoxyribonucleoside *N*-oxide derivatives in the template varied depending on the type of DNA polymerases. In the case of KF (exo$^-$), the *N*-oxide bases in the template strongly inhibit the extension of the primer. In the case of Vent (exo$^-$), the primer elongates beyond the *N*-oxide bases on the template without stopping at the next site from the oxidized damage site.

### *Ab initio* calculations of putative $C^o$–G and $A^o$–T base pairs

To discuss the base recognition ability of the modified bases of $C^o$ and $A^o$ from a theoretical viewpoint, we calculated the hydrogen bonding ability at the Watson–Crick base pairing site of $C^o$ and $A^o$. The *ab initio* calculations of the oxidized and natural base pairs at the MP2/6-31+G**//HF/6-31+G** level indicated that the hydrogen bonding geometries of the oxidized $C^o$–G and $A^o$–T base pairs were different from those of the natural C–G and A–T base pairs, respectively (40–43).

Interestingly, the optimized structure of the $C^o$–G base pair suggested that the oxygen atom of the *N*-oxide moiety can form two hydrogen bonds with the NH1 and NH2 of the guanine base (Supplementary Figure S4A). It was also suggested that this unique $C^o$–G base pair has a hydrogen bond energy of −23.6 kcal/mol that is only a little smaller by 2.2 kcal/mol than that (−25.8 kcal/mol) of the C–G base pair. The oxidized $A^o$–T base pair has two hydrogen bonds, and the hydrogen bond energy shows a minimal change of 0.4 kcal/mol (Supplementary Figure S4B).

We also found that the oxidized base pairs have slightly longer C1′–C1′ distances compared to those of the normal base pairs. The C1′–C1′ distances of the $C^o$–G and $A^o$–T base pairs were 12.3Å and 12.6Å, respectively, whereas the C1′–C1′ distance of the canonical base pair was 10.7Å. As the increase in the C1′–C1′ distance was expected to disturb the regular B-type backbone structure, it would be a major cause of the significant decrease in the $T_m$ value observed by *N*-oxidation at the center position in the ODNs, as shown in Supplementary Figure S1. In addition, in the MD simulations of DNA duplexes containing the oxidized base pair, we confirmed that the presence of the unusual base pair resulted in significant distortion of DNA duplexes (Supplementary Figures S5 and S6). The average base pair forms obtained by the MD calculation were very similar to those resulted from the *ab initio* calculation of the model base pairs. In the DNA polymerase reaction, the increased C1′–C1′ distance would be crucial for the low-incorporation efficiency of the *N*-oxide derivatives. Additionally, the inhibition of chain elongation after the incorporation of $dC^oTP$ might be due to the alteration of the base pairing geometry which would influence substrate recognition in the active site of DNA polymerases. However, in this enzymatic reaction, $dC^o$ and $dA^o$ could be selectively recognized as the complementary G and T bases at the opposite positions at the 3′-terminal site of the primer. This is probably due to the flexible 3′-terminal site that spatially allows the formation of the wider oxidized base pairs, as shown in Supplementary Figure S4.

## CONCLUSION

This study revealed that when dC and dA in DNA–DNA or DNA–RNA duplexes were replaced with $dC^o$ and $dA^o$, respectively, their thermal stability decreased significantly. From a series of $T_m$ experiments of modified DNA–DNA (or RNA) duplexes, it was also disclosed that these *N*-

oxide bases did not show selective binding ability to any canonical nucleobase at the opposite site in the complementary strand in modified DNA–DNA duplexes. To our surprise, however, the primer extensions using dC$^{o}$TP and dA$^{o}$TP in the presence of KF (exo$^{-}$) showed markedly selective incorporation of dC$^{o}$ and dA$^{o}$ into the opposite site of dG and dT, respectively, on the template DNA, as shown by the PAGE analysis. We measured single-nucleotide incorporation kinetics for KF (exo$^{-}$)-catalyzed primer extension to clarify the substrate specificity in more detail. From the data of the steady-state kinetic parameters for the single-nucleotide insertions, dC$^{o}$TP exhibited rather high-incorporation selectivity toward G in the template with at least 690-hold fidelity compared those toward the other bases. On the other hand, dA$^{o}$TP showed 13-hold fidelity toward T compared with the other bases. It was found that the incorporation efficiencies of dC$^{o}$TP and dA$^{o}$TP decreased 29 and 65 times more than those of the unmodified dCTP and dATP, respectively.

The use of Vent (exo$^{-}$) and KF (exo$^{+}$) gave results similar to those obtained by KF (exo$^{-}$) as far as the specific incorporation of the modified bases was concerned. Interestingly, Pyrobest DNA polymerase did not give single-nucleotide insertion products when dC$^{o}$TP and dA$^{o}$TP were used as the substrates. Probably, this result would be due to the strong 3′- to 5′-exonuclease activity of this enzyme.

The experiments using a mixture of dNTPs involving dC$^{o}$TP and dA$^{o}$TP suggested that chain extension could occur from the *N*-oxide bases once introduced into the 3′-terminus of the primer, but the elongation was significantly retarded at the modified position.

We also synthesized ODNs containing dC$^{o}$ or dA$^{o}$ according to our original method. These synthetic materials enabled us to determine if dNTPs can serve as the substrates in DNA-polymerase-mediated reactions when the modified bases were mis-incorporated into DNAs by duplication with dC$^{o}$TP and dA$^{o}$TP or by direct oxidation of DNAs. As a result, dGTP was found to be rather selectively chosen from the four natural dNTPs as the complementary base for C$^{o}$ in primer extensions using KF (exo$^{-}$) and Vent (exo$^{-}$) polymerases, but further chain elongation was greatly suppressed in the presence of four dNTPs. In particular, it is noteworthy that in the case of KF (exo$^{-}$), dATP was more preferentially incorporated into the opposite position of A$^{o}$ in the template than dTTP, but this misincorporation inhibited the next incorporation at the next position. A longer primer chain was observed using this enzyme upon prolongation of the reaction time when C$^{o}$ or A$^{o}$ was located in the template DNA. More interestingly, extensive chain elongation was observed when the A$^{o}$ base was located in the template DNA and Vent (exo$^{-}$) polymerase was employed.

From the theoretical point of view, the C$^{o}$–G and A$^{o}$–T base pairs could be formed as the most stable structures that have sufficient hydrogen bond energies. Molecular dynamics simulation also suggested DNA duplexes incorporating these modified bases could be kept as stable double strands although some part of the duplexes was disordered. Probably, since the oxidation of the parent bases allowed the smallest modification on the bases and the hydrogen bonding acceptor site shifted only by a distance of the N–O bond, similar Watson–Crick type hydrogen bonds can be formed between C$^{o}$ or A$^{o}$ with the complementary bases in an enzyme–primer–template complex.

Precise base recognition abilities of the *N*-oxidized bases suggest that C$^{o}$ and to a lesser extent A$^{o}$ are not highly mutagenic and only weakly lethal lesions. In contrast, 2′-deoxyribonucleoside *N*-oxide derivatives also have the property to inhibit the elongation of primer in DNA polymerase-mediated reactions. Therefore, it is believed that this property of 2′-deoxyribonucleoside *N*-oxide derivatives may induce serious errors in DNA replication if these oxidized derivatives are generated in living cells.

To clarify more biological behavior of 2′-deoxyribonucleoside *N*-oxide derivatives, it would be necessary, for example, to perform shuttle vector experiments that would involve the transfection of host cells with *N*-oxide base containing plasmids. The biochemical studies are now under way and will be reported elsewhere.

## SUPPLEMENTARY DATA

Supplementary Data are available at NAR Online.

## FUNDING

Grant-in-Aids for Scientific Research from the Ministry of Education, Culture, Sports, Science and Technology, Japan; Health Sciences Research Grants for Research on Psychiatric and Neurological Diseases and Mental Health from the Ministry of Health, Labor and Welfare of Japan, and by the global COE project (in part). Funding for open access charge: Grant-in-Aids for Scientific Research from the Ministry of Education, Culture, Sports, Science and Technology, Japan.

*Conflict of interest statement*. None declared.

## REFERENCES

1. Simandan,T., Sun,J. and Dix,T.A. (1998) Oxidation of DNA bases, deoxyribonucleosides and homopolymers by peroxyl radicals. *Biochem. J.*, **335**, 233–240.
2. Cadet,J., Delatour,T., Douki,T., Gasparutto,D., Pouget,J.P., Ravanat,J.L. and Sauvaigo,S. (1999) Hydroxyl radicals and DNA base damage. *Mutat. Res.*, **424**, 9–21.
3. Gasparutto,D., Bourdat,A.G., D'Ham,C., Duarte,V., Romieu,A. and Cadet,J. (2000) Repair and replication of oxidized DNA bases using modified oligodeoxyribonucleotides. *Biochimie*, **82**, 19–24.
4. Bjelland,S. and Seeberg,E. (2003) Mutagenicity, toxicity and repair of DNA base damage induced by oxidation. *Mutat. Res.*, **531**, 37–80.
5. Slupphaug,G., Kavli,B. and Krokan,H.E. (2003) The interacting pathways for prevention and repair of oxidative DNA damage. *Mutat. Res.*, **531**, 231–251.
6. Cadet,J., Douki,T., Gasparutto,D. and Ravanat,J.L. (2003) Oxidative damage to DNA: formation, measurement and biochemical features. *Mutat. Res.*, **531**, 5–23.
7. Brown,K.L., Adams,T., Jasti,V.P., Basu,A.K. and Stone,M.P. (2008) Interconversion of the *cis-5R,6S*- and *trans-5R,6S*-thymine

glycol lesions in duplex DNA. *J. Am. Chem. Soc.*, **130**, 11701–11710.
8. Shibutani,S., Bodepudi,V., Johnson,F. and Grollman,A.P. (1993) Translesional synthesis on DNA templates containing 8-oxo-7,8-dihydrodeoxyadenosine. *Biochemistry*, **32**, 4615–4621.
9. Purmal,A.A., Lampman,G.W., Bond,P.J., Hatahet,Z. and Wallace,S.S. (1998) Enzymatic processing of uracil glycol, a major oxidative product of DNA cytosine. *J. Biol. Chem.*, **273**, 10026–10035.
10. Kusumoto,R., Masutani,C., Iwai,S. and Hanaoka,F. (2002) Translesion synthesis by human DNA polymerase η across thymine glycol lesions. *Biochemisty*, **41**, 6090–6099.
11. Sekiguchi,M. and Tsuzuki,T. (2002) Oxidative nucleotide damage: consequences and prevention. *Oncogene*, **21**, 8895–8904.
12. Nakabeppu,Y., Sakumi,K., Sakamoto,K., Tsuchimoto,D., Tsuzuki,T. and Nakatsu,Y. (2006) Mutagenesis and carcinogenesis caused by the oxidation of nucleic acids. *Biol. Chem.*, **387**, 373–379.
13. Einolf,H.J., Schnetz-Boutaud,N. and Guengerich,F.P. (1998) Steady-state and pre-steady-state kinetic analysis of 8-oxo-7,8-dihydroguanosine triphosphate incorporation and extension by replicative and repair DNA polymerases. *Biochemistry*, **37**, 13300–13312.
14. Shimizu,M., Gruz,P., Kamiya,H., Masutani,C., Xu,Y., Usui,Y., Sugiyama,H., Harashima,H., Hanaoka,F. and Nohmi,T. (2007) Efficient and erroneous incorporation of oxidized DNA precursors by human DNA polymerase η. *Biochemistry*, **46**, 5515–5522.
15. Purmal,A.A., Bond,J.P., Lyons,B.A., Kow,Y.W. and Wallace,S.S. (1998) Uracil glycol deoxynucleoside triphosphate is a better substrate for DNA polymerase I Klenow fragment than thymine glycol deoxynucleoside triphosphate. *Biochemistry*, **37**, 330–338.
16. Ames,B.N., Shigenaga,M.K. and Hagen,T.M. (1993) Oxidants, antioxidants, and the degenerative diseases of aging. *Proc. Natl Acad. Sci. USA*, **90**, 7915–7822.
17. Cooke,M.S., Evans,M.D., Dizdaroglu,M. and Lunec,J. (2003) Oxidative DNA damage: mechanisms, mutation, and disease. *FASEB J.*, **17**, 1195–1214.
18. Lovell,M.A. and Markesbery,W.R. (2007) Oxidative DNA damage in mild cognitive impairment and late-stage Alzheimer's disease. *Nucleic Acids Res.*, **35**, 7497–7504.
19. Boveris,A. (1977) Mitochondrial production of superoxide radical and hydrogen peroxide. *Adv. Exp. Med. Biol.*, **78**, 67–82.
20. Badwey,A. and Kanovsky,M.L. (1980) Active oxygen species and the functions of phagocytic leukocytes. *Annu. Rev. Biochem.*, **49**, 695–726.
21. Winterbourn,C.C. (2008) Reconciling the chemistry and biology of reactive oxygen species. *Nat. Chem. Biol.*, **4**, 278–286.
22. Stevens,M.A., Magrath,D.I., Smith,H.W. and Brown,G.B. (1958) Purine *N*-oxides. I. Mono-oxides of aminopurines. *J. Am. Chem. Soc.*, **80**, 2755–2758.
23. Cramer,F. and Seidel,H. (1963) Studies on the formation of $N_1$-oxides of cytosine and cytosine derivatives. *Biochim. Biophys. Acta*, **72**, 157–161.
24. Delia,T.J., Olsen,M.J. and Brown,G.B. (1965) Cytosine 3-N-oxide and its rearrangement on acetylation. *J. Org. Chem.*, **30**, 2766–2768.
25. Rhaese,H.J. (1968) Chemical analysis of DNA alterations. 3. Isolation and characterization of adenine oxidation products obtained from oligo- and monodeoxyadenylic acids treated with hydroxyl radicals. *Biochim. Biophys. Acta*, **166**, 311–326.
26. Subbaraman,L.R., Subbaraman,J. and Behrman,E.J. (1969) The reaction of nucleic acid components with m-chloroperoxybenzoic acid. *Biochemistry*, **8**, 3059–3066.
27. Sako,M. and Kawada,H. (2004) A new and efficient synthetic method for $^{15}N_3$-labeled cytosine nucleosides: Dimroth rearrangement of cytidine $N_3$-oxides. *J. Org. Chem.*, **69**, 8148–8150.
28. Mouret,J.F., Odin,F., Polverelli,M. and Cadet,J. (1990) $^{32}$P-postlabeling measurement of adenine *N*-1-oxide in cellular DNA exposed to hydrogen peroxide. *Chem. Res. Toxcol.*, **3**, 102–110.
29. Mouret,J.F., Polverelli,M., Sarrazini,F. and Cadet,J. (1991) Ionic and radical oxidations of DNA by hydrogen peroxide. *Chem. Biol. Interact.*, **77**, 187–201.
30. Cadet,J. and Weinfeld,M. (1993) Detecting DNA damage. *Anal. Chem.*, **65**, 675–682.
31. Signorini,N., Molko,D. and Cadet,J. (1998) Polyclonal antibodies to adenine $N^1$-oxide: Characterization and use for the measurement of DNA damage. *Chem. Res. Toxicol.*, **11**, 1169–1175.
32. Akiyama,T., Tanaka,K., Bessho,K. and Yoneda,F. (1990) The reductive repair of adenine-1-oxide derivatives to adenine derivatives by γ-glutamylcysteinylglycine (glutathione). *Chem. Pharm. Bull.*, **38**, 2893–2895.
33. Shibutani,S., Takeshita,M. and Grollman,A.P. (1991) Insertion of specific bases during DNA synthesis past the oxidation-damaged base 8-oxodG. *Nature*, **349**, 431–434.
34. Brown,G.B., Clarke,D.A., Biesele,J.J., Kaplan,L. and Stevens,M.A. (1958) Purine *N*-oxides III. Some biological activities of adenine 1-N-oxide derivatives. *J. Biol. Chem.*, **233**, 1509–1512.
35. Brown,G.B., Levin,G. and Murphy,S. (1964) Purine *N*-oxides XII. Photochemical changes induced by ultraviolet radiation. *Biochemistry*, **3**, 880–883.
36. Montgomery,J.A. (1989) Approaches to antiviral chemotheraphy. *Antiviral Res.*, **12**, 113–132.
37. Kane,E.N. and Shuman,S. (1995) Adenosine $N_1$-oxide inhibits vaccinia virus replication by blocking translation of viral early mRNAs. *J. Virol.*, **69**, 6352–6358.
38. Tsunoda,H., Ohkubo,A., Taguchi,H., Seio,K. and Sekine,M. (2008) Synthesis and properties of DNA oligomers containing 2′-deoxynucleoside *N*-oxide derivatives. *J. Org. Chem.*, **73**, 1217–1224.
39. Xiong,A.-S., Yao,Q.-H., Peng,R.-H., Li,X., Dan,H.-Q., Chen,Z.-M. and Li,Y. (2004) A simple, rapid, high-fidelity and cost-effective PCR-based two-step DNA synthesis method for long gene sequences. *Nucleic Acids Res.*, **32**, e98.
40. Kawahara,S., Wada,T., Kawauchi,S., Uchimaru,T. and Sekine,M. (1999) Ab initio and density functional studies of substituent effects of an A-U base-pair on the stability of hydrogen bonding. *J. Phys. Chem. A*, **103**, 8516–8523.
41. Kawahara,S., Uchimaru,T., Taira,K. and Sekine,M. (2001) Ab initio evaluation of the substitution effect of the hydrogen bond energy of the Watson-Crick type base pair between 1-methyluracil and substituted 9-methyladenine derivatives. *J. Phys. Chem. A*, **105**, 3894–3898.
42. Kawahara,S., Kobori,A., Sekine,M., Taira,K. and Uchimaru,T. (2001) Theoretical study of the hydrogen bond energy of base pairs formed between substituted 1-methylcytosine derivatives and 9-methylguanine. *J. Phys. Chem. A*, **105**, 10596–10601.
43. Kawahara,S., Uchimaru,T., Taira,K. and Sekine,M. (2002) An Ab initio study of the hydrogen bond energy of base pairs formed between substituted 9-methylguanine derivatives and 1-methylcytosine. *J. Phys. Chem. A*, **106**, 3207–3212.